Plant Physiol. (1982) 69, 585–590
0032-0889/82/69/0585/06/$00.50/0

Physical Aspects of Fruit Growth

STRESS DISTRIBUTION AROUND LENTICELS

Received for publication April 21, 1981 and in revised form August, 24, 1981

KEN BROWN AND JOHN CONSIDINE
Department of Mechanical and Industrial Engineering, University of Melbourne, Parkville, Victoria, 3052, Australia (K. B.); and Horticultural Research Institute, Knoxfield, P.O. Box 174, Ferntree Gully, Victoria, 3156, Australia (J. C.)

ABSTRACT

The skin around a lenticel on a soft fruit has been modelled as a thin elastic plate with a rigid circular inclusion and applied tensile loads at the edges. A solution for the stress distribution in the skin has then been found using the linear theory of elasticity. From that solution the severity of the stress concentration and the location and form of initial cuticular failure have been deduced, the latter two being in broad agreement with observed crack initiation in the cuticle of grapes.

Splitting and cracking of fruit is a physiological disorder which occurs in many cultivated forms of soft fruits such as grape, tomato, peach, and cherry. Commonly, the site of initiation of the failure is the cuticle, and in a previous paper (2), we examined the stress distribution in the skin of soft fruit, treating the fruit skin as a pressure vessel with internal pressure. The flesh of the fruit was treated as fluid and the stress components at points on the skin of fruits of various axisymmetric shapes were calculated using the theory of thin shells. A substantial degree of success was achieved in predicting the location and nature of the failures leading to skin cracking, but no attempt was made to predict the internal pressure at which the cracking first occurred—such prediction would require some quite detailed knowledge of the mechanical properties of the skin involved.

Observations of the initial cracks in fruit skins have shown that the cracks are frequently initiated at or very near lenticels (1, 6). It would appear that the skin cannot be treated as uniform, and that the lenticel is acting as a stress concentrator. The purpose of the following work is to examine the stress distribution around lenticels and the role of that stress distribution in fruit splitting. Since measurement of the mechanical stress around a lenticel would be exceedingly difficult, the discussion is based on an analytical prediction of the stress distribution, for which analysis it has been necessary to create a simplified model of the skin and lenticel.

THE MODEL

The simplifying assumptions and their repercussions are outlined below:

(a) The lenticel and a relatively small amount of surrounding skin can be treated in isolation—*i.e.* the stress distribution close to a lenticel does not depend on the overall shape or other properties of the fruit.

This assumption is really invoking St. Venant's principle (10, p 33) and allows treatment of the lenticel and surrounding skin as a piece of shell including some kind of stress concentrator.

(b) The skin is thin, isotropic, Hookean elastic, and, remote from the lenticel, is in a state of simple bi-axial tension.

If the skin thickness and lenticel size are small compared to the radii of curvature of the shell, then the curvature may be ignored so long as the analysis is applied only to that portion of the skin which is close to the lenticel. The model then becomes that of a flat skin with lenticel, with loads in the form of bi-axial tension applied to the skin edges, at some distance from the lenticel. The choice of an isotropic, Hookean elastic solid to model the skin has been made principally because it leads to the simplest methods of solution and little is known of the mechanical properties of the skin anyway. What is known suggests that the skin is at least roughly isotropic (3, 5). Poisson's ratio ν is approximately equal to 0.25, and this figure has been adopted throughout this work. Only minor changes to the diagrams would result from another choice.

This restriction to a Hookean elastic material is perhaps not as severe as it seems since, should more complete information on the material properties become available, it would be possible to convert this elastic solution into a linear visco-elastic solution by the use of the correspondence principle (4).

Elementary theory of continuum mechanics (9, p 40) shows that there must always exist two perpendicular directions in the skin surface, in the planes of which there are no shear stresses. This is true irrespective of the nature of the material or shape of the shell and consequently, that simple bi-axial tension exists in the skin remote from the lenticel is not really an assumption at all. In an axisymmetric fruit, the stresses could be found by the methods of Considine and Brown (2). Other shapes would complicate matters, but the same principles would apply.

(c) The lenticel is circular when viewed in a direction normal to the surface of the fruit and is either much thicker or composed of material with sufficiently high Young's modulus to be considered absolutely rigid.

The underlying simplification introduced by this assumption is that, whatever loads are applied, the relative displacements of points in the skin immediately adjacent to the lenticel are trivially small when compared with the displacement of points in the skin remote from the lenticel.

(d) Attachment of the lenticel to the surrounding skin is assumed perfect. That is, failure occurs by deformation of the skin, not by breaking its bonds with the lenticel. This certainly seems to be true in the failures observed.

Thus, the model for analysis can be summarized as a flat uniform infinite Hookean plate in plane bi-axial tension with a rigid circular plug or inclusion.

ANALYSIS

Readers unfamiliar with the terms used in stress analysis should refer to the appendix.

Of the many stress analysis methods available, the one most appropriate to the problem was developed by Muskhelishvili (7). The chosen polar coordinate system of r and θ is shown in Figure 1 and the two applied loads P and Q were chosen to be in the directions $\theta = 0°$ and $\theta = 90°$, respectively. For convenience, the convention $P > Q$ has been adopted. The details of the method of solution are laborious and are not presented here. It will be evident that the solution obtained satisfies the given boundary conditions *viz.*—loads P and Q remote from the origin, and zero displacement on the circle $\rho = \frac{r}{R} = 1$, R being the lenticel radius. That the solution also satisfies the equations of elasticity (Hooke's law, equilibrium and compatibility) can be checked by straightforward but laborious methods. The solution obtained was:

$$\frac{\sigma_{rr}}{\sigma_a} = 1 + \frac{\kappa - 1}{2\rho^2} + \frac{\sigma_f}{\kappa\sigma_a}\left(\kappa + \frac{4}{\rho^2} - \frac{3}{\rho^4}\right)\cos 2\theta,$$

$$\frac{\sigma_{\theta\theta}}{\sigma_a} = 1 - \frac{\kappa - 1}{2\rho^2} + \frac{\sigma_f}{\kappa\sigma_a}\left(-\kappa + \frac{3}{\rho^4}\right)\cos 2\theta,$$

$$\frac{\sigma_{r\theta}}{\sigma_a} = -\frac{\sigma_f}{\kappa\sigma_a}\left(\kappa - \frac{2}{\rho^2} + \frac{3}{\rho^4}\right)\sin 2\theta,$$

$$\frac{u_r}{R} = \frac{(1+\nu)}{E}\rho\,\sigma_a\left[\frac{\kappa - 1}{2}\left(1 - \frac{1}{\rho^2}\right) + \frac{\sigma_f}{\kappa\sigma_a}\left(1 - \frac{1}{\rho^2}\right)\left(\kappa - \frac{1}{\rho^2}\right)\cos 2\theta\right],$$

$$\frac{u_\theta}{R} = -\frac{(1+\nu)}{E}\rho\,\sigma_a\left[\frac{\sigma_f}{\kappa\sigma_a}\left(1 - \frac{1}{\rho^2}\right)\left(\kappa - \frac{1}{\rho^2}\right)\sin 2\theta\right],$$

where

σ_{rr} = normal stress in the radial direction,

$\sigma_{\theta\theta}$ = normal stress in the tangential direction,

$\sigma_{r\theta}$ = shear stress on a face normal to the radial direction,

u_r = radial displacement,

u_θ = tangential displacement,

$$\sigma_a = \frac{P + Q}{2}$$

$$\sigma_f = \frac{P - Q}{2}$$

E = Young's modulus, ν = Poisson's ratio for the material,

and κ is a combination of elastic constants peculiar to the method. On this occasion the problem is one of plane stress (no forces perpendicular to the skin) and $\kappa = \frac{3 - \nu}{1 + \nu}$.

The above equations allow calculation of the stresses at any point defined by ρ, θ given P and Q. Mohr's circle (9, V1, p 46) can then be used to find the principal stresses σ_1 and σ_2 and their directions.

Knowing the stress state at a point one then can determine whether the material will fail at that point by the use of a yield criterion. The one chosen, variously called the maximum shear strain energy criterion, the Von Mises criterion, Henky criterion, or octahedral shear stress criterion, is the one best suited to isotopic ductile materials such as metals and plastics. It would presumably be appropriate for the cuticle but the effect of the underlying cellular structure is difficult to assess. No literature on the subject is known to the authors. The failure criterion allows the definition

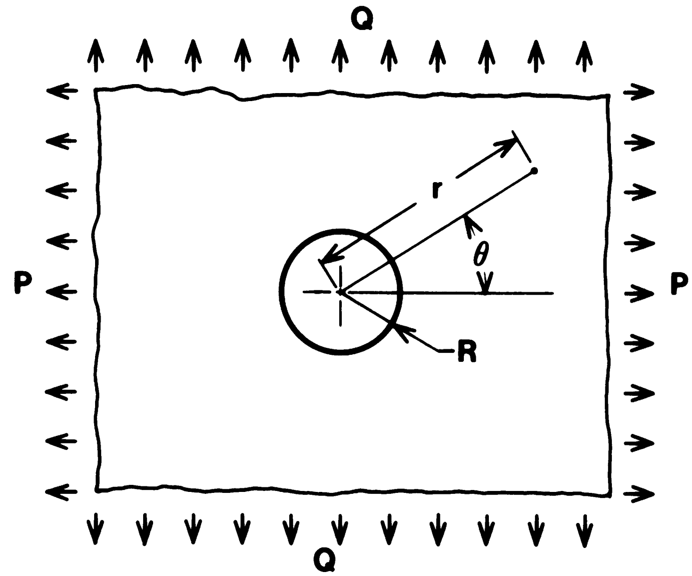

FIG. 1. The location of a point on the skin is defined by its polar coordinates r and θ, r being the radius of the point from the center of the lenticel of radius R, and θ being the angle measured counterclockwise from P, the larger of the two applied loads.

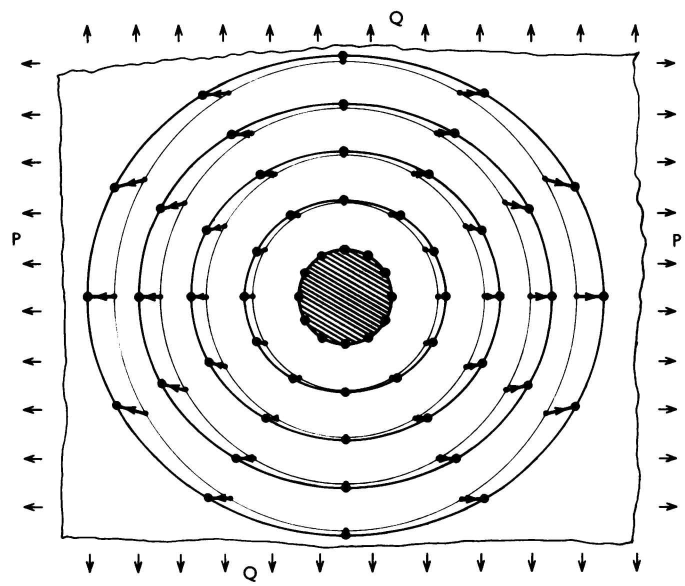

FIG. 2. Representative displacement field. Assumed: $\frac{\sigma_f}{\sigma_a} = 0.4$ $\frac{\sigma_a}{E} = 0.1$ Points on circles concentric with the lenticel when the skin is unloaded displace when the load is applied to become points on concentric ellipses.

of an equivalent stress $\bar{\sigma}$, where

$$\bar{\sigma} = \sqrt{\sigma_1^2 + \sigma_2^2 - \sigma_1\sigma_2}.$$

(In this situation the third principal stress σ_3 normal to the skin surface, is negligible.) When this equivalent stress $\bar{\sigma}$ reaches the 'Tensile yield strength' of the material, permanent deformation and consequent splitting occurs.

All of the above equations are readily programmed on a hand calculator, and some results are presented in the following figures.

Figure 2 shows a representative displacement field. All displacements calculated are relative to the lenticel. The assumed value of $\frac{\sigma_a}{E} = 0.1$ is probably quite unrealistic, but only changes the magnitude of the relative displacements, not their character. It can be shown that points on the skin, which in the undeformed state form a circle concentric with the lenticel, displace to become points on a concentric ellipse.

Figure 3 shows the distribution of equivalent stress around a 180° section of the circumference of the lenticel. Note that the distribution changes considerably with variation of $\frac{\sigma_f}{\sigma_a}$.

The equivalent stress for $\frac{\sigma_f}{\sigma_a} = 0$ ($P = Q$) is the same at all points around the lenticel. However, with P only slightly greater than $Q\left(\frac{\sigma_f}{\sigma_a} \text{ small}\right)$, a clear maximum occurs at $\theta = 0$, and with $Q = 0$ $\left(\frac{\sigma_f}{\sigma_a} = 1\right)$, four separate and distinct maxima exist at $\theta = \pm 32.9°$ and $\theta = +147.1°$.

This change in the nature of the equivalent stress distribution becomes even more apparent when one compares Figures 4 and 5, which depict contours of constant $\bar{\sigma}$. In the degenerate case $\sigma_f = 0 (P = Q)$ the contours become concentric circles, whereas

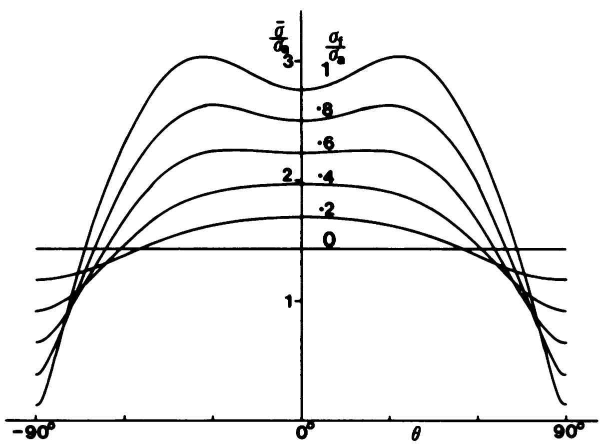

FIG. 3. Distribution of equivalent stress $\bar{\sigma}$ around the edge of one-half of the lenticel ($-90° < \theta < 90°$). When $\frac{\sigma_f}{\sigma_a}$ is small, two maxima in $\bar{\sigma}$ occur, one at $\theta = 0°$ and a similar one at $\theta = 180°$. When $\frac{\sigma_f}{\sigma_a}$ is large, a total of six maxima exist, only four of which occur on the lenticel edge. Of those four two are shown between $\theta = -90°$ and $+90°$ on the diagram, the other two occur between $\theta = 90°$ and 270° and can be found by symmetry.

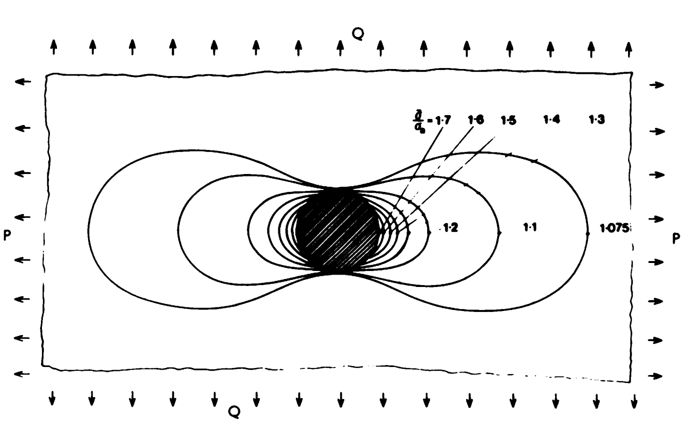

FIG. 4. Contours of constant equivalent stress $\frac{\bar{\sigma}}{\sigma_a}$. Assumed: $\frac{\sigma_f}{\sigma_a} = 0.2$.

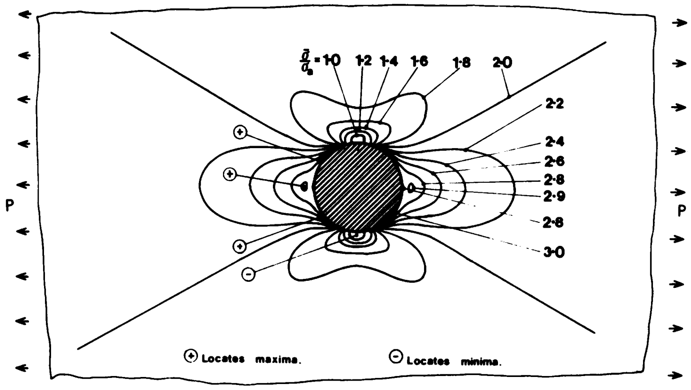

FIG. 5. Contours of constant equivalent stress $\frac{\bar{\sigma}}{\sigma_a}$. Assumed: $\frac{\sigma_f}{\sigma_a} = 0.1$.

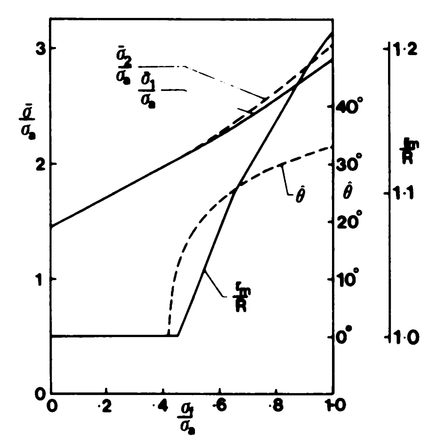

FIG. 6. Location and magnitude of the maxima in equivalent stress as functions of $\frac{\sigma_f}{\sigma_a}$. The maxima which occur on the axis $\theta = 0$ (or 180°) have equivalent stress $\frac{\bar{\sigma}}{\sigma_a}$ and are located away from the lenticel at a radius $\frac{r_m}{R}$. The maxima which occur on the lenticel edge do so at $\theta = \pm\hat{\theta}$ or $\theta = 180° + \hat{\theta}$ and have equivalent stress $\frac{\bar{\sigma}_2}{\sigma_a}$.

Figure 5 clearly shows the existence of six maxima and two minima within the field of interest. It would seem that as the ratio $P{:}Q$ is increased from near 1, the maximum at $\theta = 0$ first becomes more definite, then divides into three separate maxima, one of value $\bar{\sigma}_1$, moves along the axis $\theta = 0$ to a location $\frac{r_m}{R}$, while the other two of value $\bar{\sigma}_2$ move around the edge of the lenticel to form a symmetric pair located at $\theta = \pm\hat{\theta}$. The location $\hat{\theta}$ depends upon $\frac{\sigma_f}{\sigma_a}$. This is illustrated by Figure 6, in which the locations and values of the maxima are plotted.

Usually a failure would be expected to initiate at the location of the largest equivalent stress. Figure 6 then suggests that all cracks should initiate at the boundary of the lenticel at the location $\hat{\theta}$ appropriate to the value of $\frac{\sigma_f}{\sigma_a}$. However, on further consideration, it is suggested that this may not always be the case in practice, the reason being that assumption (b) may not be adequately satisfied very close to the lenticel edge.

Assumption (b) has been used to validate a model of the skin and lenticel in which the skin is represented as a thin plate, free to deform in the thickness direction. It is this thinning or necking which ultimately results in rupture and cracking of the skin.

However, if the lenticel is strong and rigid as we have suggested, it will restrain those deformations which would result in severe necking. The effect would be expected to influence only deformations that occur at distances within one or two skin thicknesses of the edge of the lenticel. Observation of Figure 5 indicates that the surface maximum $\bar{\sigma}_2$ is extremely local, and it may well be local enough to ensure that actual failures always occur at the maximum $\bar{\sigma}_1$ on the $\theta = 0$ axis.

Having discussed the question of where the failure should initiate, there remains the question of the direction in which the crack should propagate. This question is a particularly difficult one to answer in general, since as soon as the crack forms the stress distribution will change with the result that the direction of crack propagation will change. Nevertheless, the initiation of the crack would be expected to involve a necking process, and the thin neck would form perpendicular to the larger of the local principal stresses in the plane of the skin. Figures 7 and 8 show the 'stress trajectories' for the loadings already used in Figures 4 and 5. Stress trajectories are defined as lines which are everywhere tangent to the local principal stress directions and therefore form an orthogonal net. Thus, the initial crack, wherever it forms, would be expected to lie along the stress trajectories of the smallest principal stress.

Finally, Figure 9 shows just how much weaker than smooth unmarked skin is the skin with a lenticel present. The information is presented as a "stress concentration factor' K, defined as the ratio of the maximum equivalent stress ($\bar{\sigma}_1$ or $\bar{\sigma}_2$) to the equivalent stress at points remote from the lenticel (or, if preferred, the equivalent stress if the lenticel did not exist). Even with $P = Q$ (an equal applied load in all directions) a stress concentration factor of 1.44 applies, and failure would almost certainly occur at the

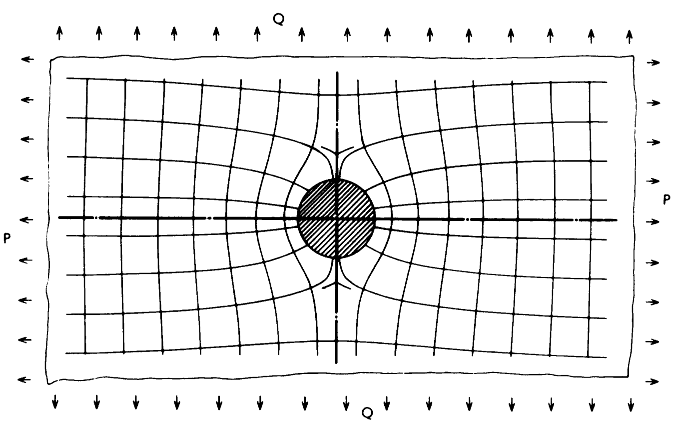

FIG. 7. Stress trajectories—lines which are everywhere in the direction of the principal stresses. Assumed: $\frac{\sigma_f}{\sigma_a} = 0.2$.

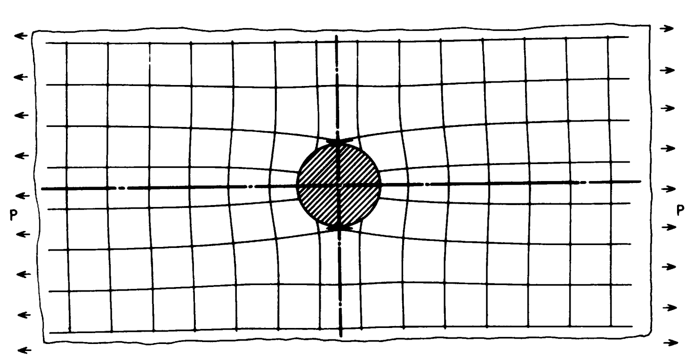

FIG. 8. Stress trajectories. Assumed: $\frac{\sigma_f}{\sigma_a} = 1.0$ (*i.e.* $Q = 0$).

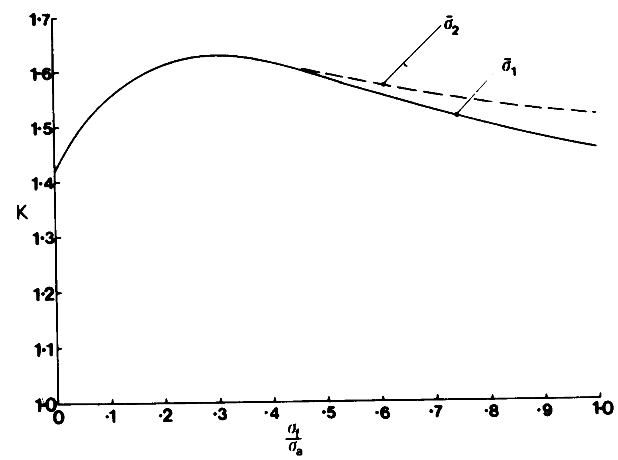

FIG. 9. Stress concentration factors K as functions of $\frac{\sigma_f}{\sigma_a}$ for the two maximum equivalent stresses $\bar{\sigma}_2$ and $\bar{\sigma}_1$.

lenticel. From the existence of the obvious maximum in the stress concentration factor at $\frac{\sigma_f}{\sigma_a} \simeq 0.30$ it could be concluded that fruit shapes which result in $Q = 0.5P$ at the most highly stressed portion of the skin would be more susceptible to cracking than are fruits which display the same equivalent stress levels, but higher or lower ratios of Q:P.

DISCUSSION

An understanding of the physical aspects of growth of plant organs requires a knowledge of the forces which attend growth and the rheological properties of the materials which constrain growth. Determination of the forces associated with growth and extension may be considered in two parts; those which determine the magnitude of the primary energy source, turgor or hydrostatic pressure, and those which translate this turgor pressure into the stresses acting at a tangent to the organ surface. Using a simplified model of a fruit, we have previously demonstrated the influence of organ geometry and accounted for five of six defined forms of fracture and fracture pattern (2). In this study we have elucidated theoretical aspects concerning the remaining form of fracture which originates in the region of lenticels.

Factors which impinge upon the arguments presented include the assumptions of a circular plug as the form of the lenticel, and the relative rheological properties of the skin and lenticel. The anatomy of lenticels in fruits of the grape is not that of a simple plug, but rather that of a conical plug extending under the cuticular membrane (8). This observation reinforces the assumption of perfect adherence of cuticular membrane and lenticel but makes it difficult to define the edge of the plug, and thus to ascertain whether in practice the failures initiate at the edge or at some defined distance from it.

Prediction of the site of initiation of cuticular failure or splitting is complex and will not necessarily be at the point or points of predicted stress maxima. At values of $\frac{P - Q}{P + Q} < 0.4$ there are two diametrically opposed maxima in line with the direction of P and at the edge of the lenticel. As stated earlier in the analysis, it is likely that the rigidity of the lenticel will prevent initiation of the necking (thinning) process involved in the mechanism of failure, and failure will occur at a distance from the lenticel sufficient to allow the necking process. At values of $\frac{P - Q}{P + Q} > 0.4$, the site should move out from the interface or at values >0.44 could also move around the edge from the direction of P. Again, the rigidity of the lenticel would probably ensure that failure is actually initiated at the maximum, in line with the direction of P, and displaced from the edge of the lenticel. This argument is supported by observations made on failure patterns around lenticels of fruits of the grape (1). In all instances observed, the failure occurred at some distance from the lenticel and was either concentric with it or was in the form of an arc which extended perpendicular to P (*cf.* Figure 7).

The results of this investigation indicate that lenticels or other rigid bodies embedded in the surface tissues act as stress concentrators with the intensity of the stress being dependent on the magnitude of the principal loads, P and Q but not upon the size of the inclusion. This general conclusion is in accord with previously published observations on fracture formation in fruits of the grape vine *Vitis vinifera*, (1, 6).

The magnitude of the stress concentrating effect achieved is predicted to be greatest ($K = 1.63$) if one of the principal stresses is twice the magnitude of the other ($Q = 0.5P$). This condition would be met on fruits with either an oblate or prolate form or near the pedicel on fruits with a relatively stiff core (2). However, a stress concentration exists even if the skin around the lenticel is loaded equally in all directions ($P = Q$) or only in one direction ($Q = 0$). These conditions result in stress concentration factors of about 1.4 and 1.5, respectively.

The conclusions reached through this study reinforce those of the previous study (2) which demonstrated the potential disadvantages of nonspherical fruit, because the presence of lenticels may further multiply the high stresses produced by certain geometries. A particular advantage may be achieved by selecting for fruit without lenticels, though this may be difficult to achieve in practice because the presence or absence of lenticels may be a species characteristic.

Lenticels have been reported to be absent from the fruits of tomatoes (*Lycopersicum esculentum*), blueberries (*Vaccinium* spp.) and persimmon (*Diospyros kaki*), but present in fruits of the grape (*Vitis* spp.) and apple (*Malus* spp.) (8, 11).

In conclusion, this analysis has demonstrated that the presence of lenticels or other rigid bodies such as sclereid masses or heavily cutinized areas of damaged tissue may in particular circumstances cause initiation or rupturing of the protective cuticular membrane and allow entry of plant pathogens.

LITERATURE CITED

1. Considine JA 1982 Physical aspects of fruit growth: cuticular fracture and fracture patterns in relation to fruit structure in *Vitis vinifera*. J Hort Sci In press
2. Considine JA, KC Brown 1981 Physical aspects of fruit growth: a theoretical analysis of the distribution of surface growth forces in fruit in relation to cracking and splitting. Plant Physiol 68: 371–376
3. Finney EE Jr 1967 Dynamic elastic properties of some fruits during growth and development. J Agric Eng Res 12: 249–256
4. Flügge W 1967 Viscoelasticity. Blaisdell, Waltham, Mass
5. Hankinson B, VNM Rao, CJB Smit 1977 Viscoelastic and histological properties of grape skins. J Food Sci 42: 632–635
6. Meynhardt JT 1964 Some studies on berry splitting of Queen of the Vineyard grapes. S Afr J Agric Sci 7: 179–186
7. Muskhelishvili NI 1973 Some Basic Problems of the Mathematical Theory of Elasticity, English, Ed 2. Translated by JRM Radok, Noordhoff, Groningen
8. Swift JG, MS Buttrose, JV Possingham 1973 Stomata and starch in grape berries. Vitis 12: 38–45
9. Timoshenko S 1955 Strength of Materials, Ed 3, Vols 1 and 2. Van Nostrand, Princeton, NJ
10. Timoshenko S, JN Goodier 1951 Theory of Elasticity, Ed 2. McGraw-Hill, New York
11. Ulrich R 1952 La Vie des Fruits. Masson et Cie, Paris.

APPENDIX

AN OUTLINE OF THE CONCEPTS OF STRESS ANALYSIS

A number of concepts, probably unfamiliar to most biologists but essential to any work on stress analysis, have been used in this study. Principally, the concepts involved are elaborations on the notion of stress, *viz.* normal, shear, principal, and equivalent stresses. In the following we have attempted to provide a brief outline of the logical development of these concepts, just sufficient to give the unfamiliar reader some idea of what the technical terms used mean. Further information is available from any of the numerous good texts on "Strength of Materials," the "Theory of Elasticity," or the "Mechanics of Solids."

The force applied to any plane area can be conveniently resolved into two components, one normal (perpendicular) to and one tangent to the plane. The normal stress on the plane is then defined as the normal component of the force divided by the area, and the shear stress is defined as the tangential component of the force divided by the area. It is important to notice that each of these two components of stress has associated with it two directions: the direction of the component of force and also the direction of the plane on which it acts (usually the direction of a plane surface on a solid body is considered to be outward along the normal to the surface). Consequently, stress is not scalar or vector in character but is a member of a more general class of quantities called tensors. The notation for stress components reflects this, the first subscript being used to indicate the direction of the plane and the second subscript being used to indicate the direction of the force component.

Almost all calculation methods find the stress components on planes which are normal to the coordinate directions. When the arbitrary choice of the coordinate system to be used is made, that choice determines the planes on which the stress components will be found. In this work, the problem is two-dimensional and the coordinate system chosen is polar. The stress components are therefore found on two mutually perpendicular planes, one normal to the radius (components σ_{rr} and $\sigma_{r\theta}$) and one normal to the tangent (components $\sigma_{\theta\theta}$ and $\sigma_{\theta r}$). However, examination of the equilibrium of a small element in rotation (10, p 4) shows that, whatever the material, $\sigma_{r\theta} = \sigma_{\theta r}$, and it is not necessary to consider $\sigma_{\theta r}$ in the analysis.

A different choice of coordinate system (say Cartesian x, y instead of polar) would produce answers representing the stress components on different planes (normal to the x and y axis). Numerically, the results would be different, yet they must represent the same state of stress—the choice of coordinates cannot affect the facts, only our representation of the facts. Mohr's circle is a simple method by which the stress components on any pair of mutually perpendicular planes can be calculated if the stress components on any other pair of mutually perpendicular planes are known. Using Mohr's circle it can be shown (9, Vol 1, p 49; 10, p 14) that at any point in the material there always exist two perpendicular planes on which the shear stresses are zero. The normal stresses on these planes are called principal stresses (σ_1, σ_2) and the forces and normals to the planes are said to be in the principal directions. Thus, there is agreement with the heuristic concept that no matter what the applied loading might be, the material at any point in a sheet is being 'stretched' in two perpendicular directions—the principal directions.

Apart from this physical interpretation, the principal stresses have particular significance because they contain all of the necessary information about the stress state of the material but, unlike the stress components such as σ_{rr}, etc., they cannot depend upon the coordinate system chosen to solve the problem. These are the very characteristics required if one wishes to predict 'failure' of the material, and any viable failure or yield criterion must be expressible in terms of these principal stresses. Many such criteria have been proposed and it is sometimes difficult to find one which adequately predicts failure of a particular material. Clearly different materials fail by different mechanisms and require different failure criteria. The one used herein is based on the premise that the strain energy (the energy contained in the material due to its deformation and recoverable as work when the loads are removed) can be separated into two parts, one due to dilatation (expansion without change of shape) and one due to distortion (change of shape without change of volume), and that the material begins to deform permanently when the strain energy of distortion reaches a limit characteristic of the material (9, Vol 2, p 451). The limit is almost invariably found using a tensile test. The straightforward approach then would be to determine the strain energy due to distortion at "failure" in a tensile test. That however is not the usual approach. Instead it is more convenient to use the failure criterion to convert the distortion strain energy found from the principal stresses into an 'equivalent stress' which can be compared directly with tensile test results. Thus, the material 'fails' when the equivalent stress reaches the stress at which a tensile test specimen fails.